The impact of nonlinear tide–surge interaction on satellite radar altimeter-derived tides

Guarneri, H.; Verlaan, M.; Slobbe, D. C.; Veenstra, J.; Zijl, F.; Pietrzak, J.; Snellen, M.; Keyzer, L.; Afrasteh, Y.; Klees, R.

DOI
10.1080/01490419.2023.2175084

Publication date
2023

Document Version
Final published version

Published in
Marine Geodesy

Citation (APA)
Guarneri, H., Verlaan, M., Slobbe, D. C., Veenstra, J., Zijl, F., Pietrzak, J., Snellen, M., Keyzer, L., Afrasteh, Y., & Klees, R. (2023). The impact of nonlinear tide–surge interaction on satellite radar altimeter-derived tides. *Marine Geodesy*, *46*(3), 251-270. https://doi.org/10.1080/01490419.2023.2175084

Marine Geodesy

ISSN: (Print) (Online) Journal homepage: https://www.tandfonline.com/loi/umgd20

The impact of nonlinear tide–surge interaction on satellite radar altimeter-derived tides

H. Guarneri, M. Verlaan, D. C. Slobbe, J. Veenstra, F. Zijl, J. Pietrzak, M. Snellen, L. Keyzer, Y. Afrasteh & R. Klees

To cite this article: H. Guarneri, M. Verlaan, D. C. Slobbe, J. Veenstra, F. Zijl, J. Pietrzak, M. Snellen, L. Keyzer, Y. Afrasteh & R. Klees (2023): The impact of nonlinear tide–surge interaction on satellite radar altimeter-derived tides, Marine Geodesy, DOI: 10.1080/01490419.2023.2175084

To link to this article: https://doi.org/10.1080/01490419.2023.2175084

Published online: 20 Feb 2023.

MARINE GEODESY
https://doi.org/10.1080/01490419.2023.2175084

The impact of nonlinear tide–surge interaction on satellite radar altimeter-derived tides

H. Guarneri[a,b], M. Verlaan[a,b], D. C. Slobbe[c], J. Veenstra[b], F. Zijl[b], J. Pietrzak[d], M. Snellen[e], L. Keyzer[d], Y. Afrasteh[c], and R. Klees[c]

[a]Delft Institute of Applied Mathematics, Faculty of Electrical Engineering, Mathematics and Computer Science, Delft University of Technology, Delft, The Netherlands; [b]Environmental Hydrodynamics & Forecasting, Marine and Coastal Systems, Deltares, Delft, The Netherlands; [c]Department of Geoscience & Remote Sensing, Faculty of Civil Engineering and Geosciences, Delft University of Technology, Delft, The Netherlands; [d]Department of Hydraulic Engineering, Faculty of Civil Engineering and Geosciences, Delft University of Technology, Delft, The Netherlands; [e]Department of Control and Operations, Faculty of Aerospace Engineering, Delft University of Technology, Delft, The Netherlands

ABSTRACT

Both empirical and assimilative global ocean tidal models are significantly more accurate in the deep ocean than in shelf and coastal waters. In this study, we answered whether this is due to the quality of the models used to reduce tide and surge or the general approach to treat tide and surge as two separate components of the water level obtained from stand-alone models, which ignores the nonlinear tide–surge interaction. In doing so, we used tide gauge observations as partially synthetic altimeter time series, tide–surge water-level time series obtained with the 2D Dutch Continental Shelf Model – Flexible Mesh (DCSM), and tide and surge water-level time series obtained using the DCSM, FES2014 (FES) and the Dynamic Atmospheric Correction (DAC) product. Expressed in the root-sum-square (RSS) of the eight main tidal constituents, we obtained a reduction $> 50\%$ when removing the DCSM tide–surge water levels compared to when we removed the sum of the DCSM tide and DCSM surge water levels. The RSS obtained in the latter case was only 3.3% lower than with FES and DAC. We conclude that the lower tidal estimates accuracy in shelf-coastal waters derives from the missing nonlinear tide–surge interactions.

ARTICLE HISTORY
Received 3 October 2022
Accepted 30 December 2022

KEYWORDS
Harmonic analysis; satellite radar altimetry; shallow waters; tides; tide–surge interactions; variance reduction

Introduction

Satellite radar altimeter data have been the primary reason for the major improvements in global ocean tide models over the past decades (Shum et al. 1997; Andersen 1999; Stammer et al. 2014; Zaron and Elipot 2021).

CONTACT H. Guarneri h.guarneri@tudelft.nl Delft Institute of Applied Mathematics, Faculty of Electrical Engineering, Mathematics and Computer Science, Delft University of Technology, Delft, Netherlands

These improvements are marked by the assessment of Stammer et al. (2014). For both empirical and assimilative models (as defined in Stammer et al. (2014)), the improvements in terms of the root-sum-square (RSS) differences with respect to tide observations for the eight major constituents (M2, S2, N2, K2, K1, O1, P1, and Q1) are approximately 60% for pelagic waters and $>70\%$ for shelf and coastal waters. These are significant improvements. However, even though the ratio will vary from place to place, *the root-sum-square differences between tide observations and the best models for eight major constituents are approximately 0.9, 5.0, and 6.5 cm for pelagic, shelf, and coastal conditions, respectively* (Stammer et al. 2014). In other words, estimating these eight constituents from altimeter data is apparently more difficult in shelf and coastal waters. This increased difficulty raises the question: why is this the case?

We have not found a study that provides an explicit answer to this question. We can, however, distil several explanations from various publications (Andersen 1999; Andersen et al. 2006; Ray, Egbert, and Erofeeva 2011). Andersen (1999) points out that, unlike the deep ocean, the dynamics in shallow waters become nonlinear, and the tidal spectrum is complicated. These nonlinearities cause : compound and overtides (also called shallow-water tides), interaction of tides with nontidal processes, and dampening of weaker constituents in the presence of the tidal currents of stronger constituents (Ray, Egbert, and Erofeeva 2011). To properly disentangle even weak nonlinear effects with their multiplicity of additional constituents (i.e. the shallow-water constituents need to be included in the functional model to make sure the model is correct) requires much more data than in linear regimes (Ray, Egbert, and Erofeeva 2011). However, here limitations arise from the sampling of the signal which is the second issue Andersen (1999) points out. The repeat period of 9.9156 days for the TOPEX/Poseidon and Jason (TPJ) satellites is much longer than most tidal periods. This causes aliasing, which makes the period of tidal constituents appear much longer. To separate the constituents, long time series are needed. The addition of the shallow-water constituents imposes even more restrictions. Depending on the orbit of the satellite(s) to be used, it may even be impossible to estimate some shallow-water constituents. In addition, and this is the third issue pointed out by Andersen (1999), the *shallow-water constituents generally have a small amplitude*. Small compared to the noise and nontidal signals in the altimeter data. The accuracy of altimeter data in coastal waters is lower (e.g. Vignudelli et al. 2011, 2019) due to land contamination of the waveforms and the lower accuracy of corrections for (i) wet and dry troposphere, and (ii) sea state and meteorological-induced effects. More important, however, is the nontidal sea-level variability close to the aliased tidal constituents. According to Andersen (1999), this is the limiting factor that

determines which shallow-water constituents can be resolved from altimeter data.

A commonly applied strategy to suppress the impact of nontidal sea-level variability, as well as unresolved tides, is to remove model-derived estimates of tide and surge before the tidal analysis is conducted. Removing the tides means that only the residual tidal amplitudes and phases are estimated. For example, Cheng and Andersen (2011) subtracted the tides from FES2004 [Finite Element Solutions (Lyard et al. 2006)] to produce the DTU10 tide model, whereas Hart-Davis et al. (2021) removes both the updated FES2014 (Lyard et al. 2021) and the dynamic atmospheric correction [DAC (Carrère and Lyard 2003; Carrère et al. 2011, Carrère, Faugère, and Ablain 2016)] to produce the EOT20 tide model. *In treating the tide and nontidal sea-level variability as independent, however, any nonlinear interaction is ignored.* Interactions between the tide and nontidal components have been reported for many places around the world (e.g. Proudman 1955a, 1955b; Prandle and Wolf 1978; Johns et al. 1985; Horsburgh and Wilson 2007; Zhang et al. 2010; Idier et al. 2012, 2019; Arns et al. 2020). Nonlinear interactions introduce phase alterations of the tidal signal while vice versa the tide modulates the nontidal signal. Because of this, it appears that the highest observed surge (defined as the difference between observed and tidal water levels) occurs around mid-tide or low tide rather than at the time of high water.

In this study, *we will answer the question of whether it is the quality of the tide and surge models that limits the accuracy of the altimeter-derived major tides or whether it is ignoring the nonlinear interactions?* This question is important. Indeed, in the case of the latter, a different type of model is needed to suppress the impact of nontidal signals and nonresolvable tides. Rather than relying on stand-alone models for the separate contributors, a 'total water-level model' is needed (or at least one that includes the most important drivers). At the same time, we have the prospect that something can be gained from altimeter data in mapping ocean tides in shelf and coastal waters.

To answer our research question, we use partially synthetic altimeter time series. These are obtained by resampling an offshore tide gauge record acquired in the southern North Sea superimposed with white noise to a time series with a sampling interval corresponding to the repeat period of the TPJ satellites. The study area is selected because (i) it is composed of many shallow-water tidal constituents, (ii) we have access to a high-resolution tide–surge model (here, tide and surge are the most important drivers for fast sea-level variations), (iii) the area of interest is known for its nonlinear interactions (Prandle and Wolf 1978), and (iv) we know what tidal constituents need to be included in the analysis to get a proper

description of the tide. Partially synthetic data are used since our study area did not comprise a tide gauge for which a sufficiently long record is available almost underneath a TPJ track. This is needed to have ground truth data for validation. In addition, it allows obtaining rigorous estimates of the uncertainty, as we can generate an ensemble of time series on which to perform the analysis.

The paper is organized as follows. Sect. 2 describes (i) the models used to apply corrections for tide and/or surge, or tide–surge water-level variability, (ii) the used tide gauge record, (iii) the method applied to generate the partially synthetic altimeter time series, (iv) the way the tidal analyses are conducted, and (v) the way the results are validated. In Sect. 3, we present, analyze, and discuss all results. Finally, we conclude by summarizing the main findings of the paper in Sect. 4.

Methods and Data

Tide, Surge, and Tide–Surge Water-Level Corrections

Corrections for tide, surge, and tide–surge water-level variability are obtained from different models. Here, the models will be briefly introduced.

FES2014

The FES2014 model is the latest publicly available version of the Finite Element Solution (FES) tide model (Lyard et al. 2021). It is a so-called 'assimilative model', i.e. the atlas is computed using a hydrodynamic model that is coupled to a data assimilation code. The data being assimilated include altimeter data from various satellite missions, 600 coastal and deep ocean tide gauges, and bottom pressure recorders. The atlas includes 34 tidal constituents that are provided on a regular 1/16° resolution. Note that only 15 of them are adjusted by data assimilation. In the assessment conducted by Zaron and Elipot (2021), the FES2014 model had the best performance near the coasts and in shallow water compared to TPXO9A (Egbert and Erofeeva 2002) and GOT410 (Ray 1999). In deep water, the accuracy of the three models is essentially indistinguishable for the eight major constituents. For a comprehensive validation of the model, we also refer to Lyard et al. (2021).

In our analyses, we use the tidal prediction software associated with the FES atlas https://bitbucket.org/cnes_aviso/fes/src/master/ (last access: 12 July 2022) to produce tidal water levels at the epochs tide gauge/altimeter measurements are available. In case, we need to restore the FES amplitudes

and phases, we restore the ones estimated with the HATYAN software package from a 10-min time series (see Sect. 2.4).

Dynamic Atmospheric Correction

The dynamic atmospheric correction is a gridded product delivered by Aviso+ (LEGOS/CNRS/CLS 1992). The 6-hourly, $0.25^\circ \times 0.25^\circ$ grids describe the ocean response to atmospheric wind and pressure forcing computed using the Mog2D barotropic model (Carrère and Lyard 2003; Carrère, Faugère, and Ablain 2016) for high frequencies (i.e. less than 20 days), and the inverted barometer correction (Ponte 2006) for lower frequencies.

We use bilinear interpolation to produce a 6-hourly time series at the Europlatform tide gauge location. Linear interpolation is used to interpolate the time series to the epochs tide gauge/altimeter measurements are available.

The Dutch Continental Shelf Model

The 2D Dutch Continental Shelf Model – Flexible Mesh (DCSM, (Zijl and Groenenboom 2019)) is the successor of the version in Zijl, Verlaan, and Gerritsen (2013) and Zijl, Sumihar, and M. Verlaan (2015). The model describes the tide–surge water-level variability for the northwest European continental shelf between 15°W to 13°E and 43°N to 64°N by solving the depth-integrated shallow-water equations for hydrodynamic modeling of free-surface flows (Leendertse 1967; Stelling 1984). In doing so, the nonlinear tide–surge interaction is accounted for. Contrary to the previous version, it uses the Delft3D Flexible Mesh Suite (or D-HYDRO Suite) that allows for the use of unstructured grids (Deltares 2022). For this model, the minimum grid size is approximately 840×930 m in Dutch waters. To reduce the uncertainty of the bottom roughness, an automated calibration using the 'Doesn't Use Derivative' algorithm (Ralston and Jennrich 1978) has been performed. In doing so, all 2017 data from 195 tide gauges were used (including the Europlatform tide gauge used in this study). Here, extra weight in the cost function has been given to the Dutch coastal tide gauges, since the model is primarily intended to obtain an accurate water-level representation in Dutch coastal areas.

At the northern, western, and southern open boundaries, water-level boundary conditions are applied. When modeling the tide–surge water levels, they are composed of the sum of the astronomical water levels and the surge. The tides are obtained from a harmonic expansion of 32 tidal constituents retrieved from the global ocean tide model FES2012 (Carrère et al. 2013) supplemented with the solar annual Sa constituent obtained from an

earlier version of the model. The surge at the open boundaries is approximated by the time- and space-dependent inverse barometer correction. Also, in the model domain, the tidal potential is simulated and accounts for a smaller part of the tides, compared to the tides forced from the open boundaries.

In our simulations, we force the model by (i) both tidal and meteorological (i.e. atmospheric wind and pressure) forcing, (ii) tidal forcing only, and (iii) meteorological forcing only. The obtained 10-min water-level time series will be, respectively, referred to as the 'DCSM tide–surge', 'DCSM tide', and 'DCSM surge' water-level time series. The difference between the DCSM tide–surge water levels and the sum of the DCSM tide and DCSM surge water levels is the adjustment of the water level by the nonlinear tide–surge interaction. When included, time- and space-varying atmospheric wind and pressure forcings are obtained from the ECMWF's ERA5 reanalysis dataset (Hersbach et al. 2020).

The Europlatform Tide Gauge Record

The tide gauge record used in this study is acquired at Europlatform, an offshore structure located in the southern North Sea that serves as a beacon for shipping and as a measurement platform (see Figure 1 for the location). The record starts in January 1983 and has a sampling interval of 10 min. In this study, we use all data from 1 January 1992, to 1 January 2017. Visual inspection of the record reveals some anomalous data (see Table 1), which were removed. We also shifted all measurement epochs before January 2000 by 5 min. Observations before this date were an average of the previous 10 min, while after this date the epochs became centered with respect to the averaging period. In using only data acquired before 1 January 2017, none of the data being used to calibrate the bottom friction in the DCSM

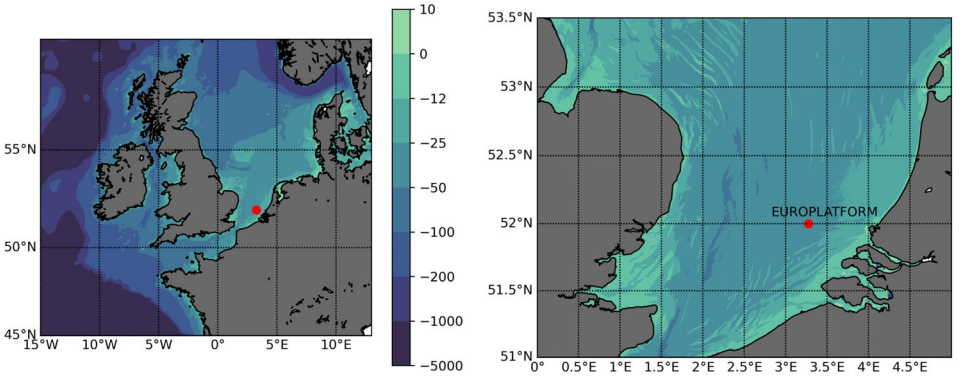

Figure 1. Location of the Europlatform tide gauge. In the background, we show the bathymetry (in meters). Source: Authors. https://emodnet.ec.europa.eu/en/copyright-notice

Table 1. Periods for which anomalous data were removed from the Europlatform tide gauge record.

Start	End
31 December 1994 23:10:00	2 January 1995 23:10:00
24 June 2004 13:00:00	24 June 2004 21:00:00
1 December 2007 16:30:00	1 December 2007 20:30:00
29 January 2010 12:00:00	2 February 2010 13:0:00
15 January 2008 13:30:00	18 January 2008 2:50:00
22 September 2009 12:20:00	22 September 2009 12:20:00
22 September 2009 15:10:00	22 September 2009 15:10:00
24 September 2009 3:30:00	24 September 2009 3:30:00

Table 2. Set of RWS constituents.

Category	Constituents
Long-period	A0, **SA**, SM
Diurnal	**Q1**, **O1**, M1C, **P1**, **S1**, **K1**
Semi-diurnal	3MKS2, 3MS2, OQ2, MNS2, 2ML2S2, NLK2, MU2, **N2**, NU2, MSK2, MPS2, **M2**, MSP2, MKS2, LABDA2, 2MN2, **T2**, **S2**, **K2**, MSN2, 2SM2, SKM2
Third-diurnal	NO3, 2MK3, 2MP3, SO3, MK3, SK3
Fourth-diurnal	4MS4, 2MNS4, 3MS4, MN4, 2MLS4, 2MSK4, **M4**, 3MN4, MS4, MK4, 2MSN4, S4
Fifth-diurnal	MNO5, 3MK5, 2MP5, 3MO5, MSK5, 3KM5
Sixth-diurnal	3MNS6, 2NM6, 4MS6, 2MN6, 2MNU6, 3MSK6, M6, MSN6, MKNU6, 2MS6, 2MK6, 3MSN6, 2SM6, MSK6
Seventh-diurnal	2MNO7, M7, 2MSO7
Eighth-diurnal	2(MN)8, 3MN8, M8, 2MSN8, 2MNK8, 3MS8, 3MK8, 2(MS)8, 2MSK8
Ninth-diurnal	3MNK9, 4MK9, 3MSK9
Tenth-diurnal	4MN10, M10, 3MSN10, 4MS10, 2(MS)N10, 3M2S10
Eleventh-diurnal	4MSK11
Twelfth-diurnal	M12, 4MSN12, 5MS12, 4M2S12

The bold ones are included in the EOT set (see Sect. 2.4).

(all data acquired in 2017) are used in our analysis. Note that the Europlatform data have not been used to generate FES2014 (Lyard et al. 2021, Figure 11).

To describe the tides at this location, a set of 95 constituents has been determined by Rijkswaterstaat (RWS). RWS is part of the Dutch Ministry of Infrastructure and Water Management and is responsible for the tide gauge network in the Netherlands. We refer to Table 2 for an overview of the constituents being included in this set.

Step 1: Partially Synthetic Altimeter Time Series Generation

The ensemble of N altimeter time series used in the analysis is generated by resampling the Europlatform tide gauge record to a time series from 1992 to 2017 with a sampling interval corresponding to the revisit period of the TPJ altimeters, i.e. 9.915 days. Each successive time series of the ensemble has a start time that is $9.915/N$ days later than the previous one. In this study, N is set to 100. Note that 15 of them lack 2 samples due to the data editing described in Sect. 2.2, while 62 lack just one sample. Altimeter noise is superimposed by adding white noise with a standard

deviation (SD) of three centimeters which express the uncertainty associated with processing and corrections defined in mission specification and confirmed by Ponte, Wunsch, and Stammer (2007).

Step 2: Tidal Analysis

The tidal analysis is based on a harmonic analysis of the *residual* water-level time series, i.e. the observed water levels minus the model-derived tide and/or surge water levels, or the model-derived tide–surge water levels. To obtain the full amplitudes and phases, we restore the amplitudes and phases estimated from a 10-min times series of the signal subtracted in the remove-step. Note that in this study the radiational tides (i.e. tides caused by atmospheric conditions and solar forcing) are considered as part of the tidal signal. Hence, if the surge water level is removed, we restore the contributions at the tidal frequencies in this signal.

Two sets of constituents are used to parameterize the residual water levels: (i) the 17 constituents (i.e. 2N2, J1, K1, K2, M2, M4, MF, MM, N2, O1, P1, Q1, S1, S2, SA, SSA, and T2) used by Hart-Davis et al. (2021) plus A0 (referred to as the 'EOT set'); and (ii) all 95 constituents included in the RWS set (see Table 2) except MNO5. MNO5 is not estimated because its alias period is too close to the one of 2ML2S2. Note that the 2N2, J1, MF, MM, and SSA constituents included in the EOT set are not in the RWS set.

The analysis is conducted using the HATYAN package (Veenstra 2022), an open-source, Python-based software package for harmonic tidal analysis and prediction owned by RWS and developed and maintained by Deltares. It is repeated for all N time series that are part of the ensemble. In the validation, we use the ensemble mean. To quantify the uncertainty, we use the standard deviation of the ensemble.

Step 3: Validation

Validation of the results is conducted by comparing the ensemble mean of the estimated amplitudes and phases to the true ones, i.e. the ones being estimated from the full observed tide gauge record. In doing so, we will compute the vector differences (VD) for all constituents being estimated. The VD is defined as (Le Provost et al. 1995):

$$\mathrm{VD} = \sqrt{(A_0 \cos g_0 - A_m \cos g_m)^2 + (A_0 \sin g_0 - A_m \sin g_m)^2}, \tag{2.1}$$

where A and g represent the amplitude (in centimeters) and phase (in degrees), and the subscripts 0 and m indicate whether it is the true or estimated one, respectively.

In this study, tide, surge, and tide–surge corrections from different sources will be considered. As such, the restore-step will differ for each scenario. Table 3 presents the scenarios and describes for each of them how the quantities are defined based on which the VDs are computed. Here, h represents the water level. The sub- and superscripts specify what part of the water level is referred to (i.e. total, tide, surge, or tide–surge) and the source from which it is obtained (obs (observed), FES, DAC, or DCSM). The hat ($\hat{}$) and tilde ($\tilde{}$) indicate the set of amplitudes and phases estimated from the full (10-min) and altimeter (9.915-day) time series, respectively, while Δ refers to their difference.

To summarize the results, we will present the VDs of the eight major tidal constituents (computed as the mean over the ensemble), their root-sum-square (RSS) that we refer to as the 'RSS8', and the RSS value computed over all constituents except A0 included in the analysis. We refer to the latter as the 'RSS17' or 'RSS93' (depending on the set of constituents being used in the analysis). Note that the RSS values are computed as the mean over the N RSS values computed for all ensemble members. The uncertainties for the individual constituents are the standard deviations of the N VDs, while the corresponding RSS values are the standard deviations of the N RSS values.

Results and Discussion

To organize the results and discussion, this section is divided into three parts. First, we will assess the quality of the various tide, surge, and tide–surge corrections at the Europlatform location. Second, we will assess the impact of reducing the water-level variability by applying the corrections on the accuracy of the altimeter-derived tides. Finally, we will present and discuss the need to account for the nonlinear tide–surge interaction in

Table 3. Overview of the different scenarios regarding the corrections applied to the observed water levels prior to the harmonic analysis.

Scenario	Validation
No correction	$\hat{h}^{\text{obs}}_{\text{total}} - \tilde{h}^{\text{obs}}_{\text{total}} = \Delta h^{\text{obs}}_{\text{total}}$
DAC	$\hat{h}^{\text{obs}}_{\text{total}} - (\tilde{h}^{\text{obs}}_{\text{total}} - \tilde{h}^{\text{DAC}}_{\text{surge}} + \hat{h}^{\text{DAC}}_{\text{surge}}) = \Delta h^{\text{obs}}_{\text{total}} - \Delta h^{\text{DAC}}_{\text{surge}}$
FES tide	$\hat{h}^{\text{obs}}_{\text{total}} - (\tilde{h}^{\text{obs}}_{\text{total}} - \tilde{h}^{\text{FES}}_{\text{tide}} + \hat{h}^{\text{FES}}_{\text{tide}}) = \Delta h^{\text{obs}}_{\text{total}} - \Delta h^{\text{FES}}_{\text{tide}}$
DAC + FES tide	$\hat{h}^{\text{obs}}_{\text{total}} - (\tilde{h}^{\text{obs}}_{\text{total}} - \tilde{h}^{\text{DAC}}_{\text{surge}} - \tilde{h}^{\text{FES}}_{\text{tide}} + \hat{h}^{\text{DAC}}_{\text{surge}} + \hat{h}^{\text{FES}}_{\text{tide}}) = \Delta h^{\text{obs}}_{\text{total}} - \Delta h^{\text{DAC}}_{\text{surge}} - \Delta h^{\text{FES}}_{\text{tide}}$
DCSM surge	$\hat{h}^{\text{obs}}_{\text{total}} - (\tilde{h}^{\text{obs}}_{\text{total}} - \tilde{h}^{\text{DCSM}}_{\text{surge}} + \hat{h}^{\text{DCSM}}_{\text{surge}}) = \Delta h^{\text{obs}}_{\text{total}} - \Delta h^{\text{DCSM}}_{\text{surge}}$
DCSM tide	$\hat{h}^{\text{obs}}_{\text{total}} - (\tilde{h}^{\text{obs}}_{\text{total}} - \tilde{h}^{\text{DSCM}}_{\text{tide}} + \hat{h}^{\text{DCSM}}_{\text{tide}}) = \Delta h^{\text{obs}}_{\text{total}} - \Delta h^{\text{DCSM}}_{\text{tide}}$
DCSM surge + DCSM tide	$\hat{h}^{\text{obs}}_{\text{total}} - (\tilde{h}^{\text{obs}}_{\text{total}} - \tilde{h}^{\text{DCSM}}_{\text{surge}} - \tilde{h}^{\text{DCSM}}_{\text{tide}} + \hat{h}^{\text{DCSM}}_{\text{surge}} + \hat{h}^{\text{DCSM}}_{\text{tide}}) = \Delta h^{\text{obs}}_{\text{total}} - \Delta h^{\text{DCSM}}_{\text{surge}} - \Delta h^{\text{DCSM}}_{\text{tide}}$
DCSM tide–surge	$\hat{h}^{\text{obs}}_{\text{total}} - (\tilde{h}^{\text{obs}}_{\text{total}} - \tilde{h}^{\text{DSCM}}_{\text{tide\&surge}} + \hat{h}^{\text{DCSM}}_{\text{tide\&surge}}) = \Delta h^{\text{obs}}_{\text{total}} - \Delta h^{\text{DCSM}}_{\text{tide\&surge}}$

For each scenario, the quantities are defined on the basis of which the VDs are calculated.

correcting the observed water levels for tide and surge. All scenarios regarding the corrections applied to the observed water levels prior to the harmonic analysis are defined in Table 3.

The Quality of the Tide, Surge, and Tide–Surge Corrections at Europlatform

The quality of the exploited corrections at Europlatform is assessed by the extent to which they explain the observed water-level variability (see Table 4). For the models used to compute the tide corrections, we also analyze the vector differences (VD) for the eight major constituents and the root-sum-square (RSS) differences (see Table 5 and Figures 2 and 3). Remember that tides from the DCSM are obtained by either applying a harmonic analysis to the tide–surge water levels (Scenario 'DCSM tide–surge') or by forcing the model with tidal forcing only (Scenario 'DCSM tide'). From these results, we observe:

Table 4. Statistics of (i) the observed total water levels at the Europlatform tide gauge for the time span 1 January 1992 to 1 January 2017, and (ii) the residual water levels after applying various corrections for tide, surge, and tide–surge water level.

Scenario	SD	Var. reduction	mean	5%	25%	50%	75%	95%
Signal	61.37	0%	2.15	−86.00	−48.00	−6.00	53.50	103.00
DAC	58.80	8.20%	6.40	−76.62	−43.04	−3.45	58.17	103.60
FES tide	23.39	85.48%	2.25	−31.30	−12.10	0.30	14.10	43.00
DAC + FES tide	15.00	94.02%	6.49	−17.32	−3.41	6.12	16.04	31.66
DCSM surge	58.55	8.98%	0.01	−82.21	−49.37	−9.86	51.67	97.01
DCSM tide	21.63	87.58%	−1.34	−30.34	−13.90	−4.11	8.08	37.59
DCSM surge + DCSM tide	11.73	96.35%	−3.49	−23.34	−10.27	−3.09	3.77	14.86
DCSM tide–surge	6.17	98.99%	−2.85	−12.34	−6.97	−3.15	1.03	7.68

The columns '5%'–'95%' represent percentiles. The percentages in the column 'Var. reduction' indicate the reduction in variance (Var) compared to the variance of the observed water levels. All other numbers are in centimeters. Note that, all corrections are computed/interpolated at the epochs of the Europlatform tide gauge record. The record includes 1, 278, 518 samples.

Table 5. The numbers corresponding to 'Signal' represent the amplitudes of the eight major tidal constituents at Europlatform, their RSS ('RSS8'), and the RSS17 or RSS93 value (see Sect. 2.5).

Scenario	Q1	O1	P1	K1	N2	M2	S2	K2	RSS8	RSS17	RSS93
Results for EOT constituent set											
Signal	3.77	11.29	3.29	8.17	11.61	73.64	18.04	5.34	78.30	79.38	
FES tide	0.40	0.52	0.55	0.39	0.62	1.77	0.69	0.51	2.26	8.28	
DCSM tide	0.08	0.24	0.39	0.74	0.29	3.58	0.72	0.23	3.78	5.99	
DCSM tide–surge	0.06	0.30	0.29	0.56	0.25	1.59	0.93	0.26	2.00	3.47	
Results for RWS constituent set											
Signal	3.76	11.29	3.29	8.17	11.60	73.65	18.04	5.34	78.30		80.96
FES tide	0.40	0.52	0.55	0.39	0.62	1.77	0.69	0.51	2.27		13.57
DCSM tide	0.08	0.24	0.38	0.74	0.29	3.57	0.72	0.23	3.76		6.66
DCSM tide–surge	0.06	0.30	0.29	0.56	0.25	1.58	0.93	0.26	1.99		4.01

For the other scenarios, the numbers represent the VDs for the eight major tidal constituents, their RSS value, and the RSS17 or RSS93 values (depending on whether the EOT set or RWS set of constituents is used in the harmonic analyses, see Sect. 2.4). All values are in centimeters and represent the mean over the N ensemble members.

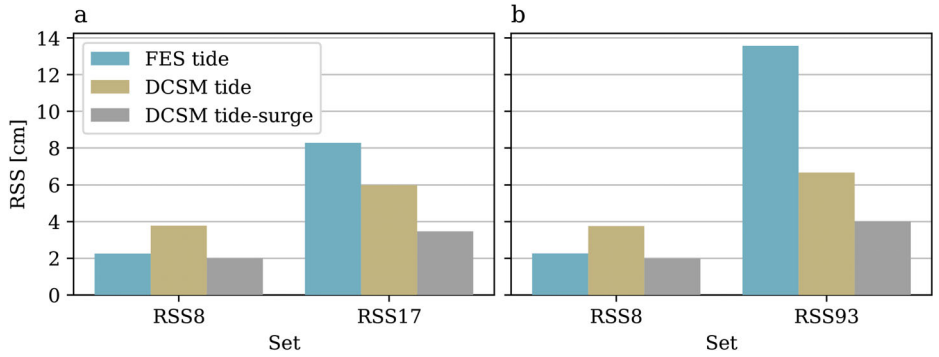

Figure 2. RSS from priors for the (a) EOT set and (b) RWS set. For the exact values, we refer to Table 5.

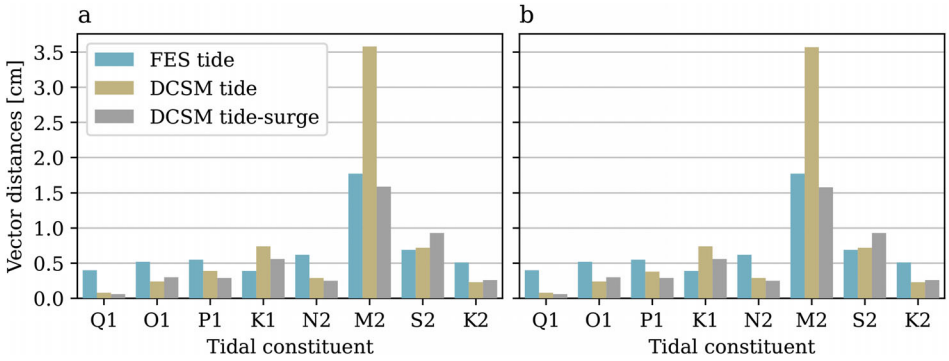

Figure 3. Prior's VDs for the 8 main tidal constituents for the (a) EOT set and (b) RWS set. For the exact values, we refer to Table 5.

- The extent to which 'FES tide' and 'DCSM tide' explain the observed water-level variability is quite similar. In terms of SD, the signal reduces from 61.37 to 23.39 cm (FES tide) and 21.63 cm (DCSM tide). For both scenarios, this implies a variance reduction of $> 85\%$.
- Because tides are the largest contributor to water-level variability in the North Sea, a correction for only the surge hardly reduces the variance (8.2% for 'DAC' and 8.98% for 'DCSM surge'). Combined with the tide, however, there is a further reduction in the SD of 8.39 cm (DAC + FES tide) and 9.90 cm (DCSM surge + DCSM tide). The difference in reduction of the SD between 'DAC + FES tide' on the one hand and the linear combination of 'DCSM surge' and 'DCSM tide' on the other hand is again relatively small, only 3.27 cm.
- Correcting the observed water levels for the DCSM-derived tide–surge water levels (DCSM tide–surge) yields the largest variance reduction; nearly 99%. The SD of the obtained residual water levels is 6.17 cm, which is 5.56 cm lower than the SD obtained when correcting the water levels using the linear combination of 'DCSM surge' and 'DCSM tide'.

- The VDs (and hence RSS8) obtained using the EOT and RWS constituent sets are identical at the millimeter level.
- The VDs of the eight major tidal constituents for both scenarios in which tides are obtained from DCSM compared to those from FES, are lower for Q1, O1, P1, N2, and K2, but higher for K1 and S2. For M2, the VD is substantially (1.8 cm) higher for 'DCSM tide', and slightly lower (0.19 cm) for 'DCSM tide–surge'. The RSS8 is comparable for 'FES tide' and 'DCSM tide–surge', but substantially higher for 'DCSM tide'. The latter is primarily caused by the higher VD for M2.
- In terms of RSS17 and RSS93, both scenarios in which tides are obtained from DCSM outperform the scenario 'FES tide'. In case the RWS constituent set is used in the tidal analysis, this result is obvious. Indeed, most constituents included in this set are not included in the FES tidal atlas. As such, their VDs represent the magnitude of these constituents.

The better performance of FES2014 in representing the S2 constituent compared with the S2 obtained for the 'DCSM tide–surge' scenario is remarkable because both the latter as well as the observation-derived value contain the atmospheric contribution.

We would like to stress that this study does not aim to demonstrate the performance of the DCSM relative to what is offered by FES2014 and DAC. Indeed, besides the fact that these are completely different models developed for different applications, the comparison of the performances is obscured by the fact that the Europlatform tide gauge record, among other ones, has been used to calibrate the DCSM model. Even though it concerns data that are not used in our analysis (in the calibration data were used acquired in 2017, while we use data up to 2017), the model representation of the tide has also changed outside the period over which calibration was conducted. The key takeaway from these results is that a significantly larger part of the observed water-level variability can be explained in case the nonlinear tide–surge interaction is taken into account.

The Impact of Reducing the Water-Level Variability on the Accuracy of Altimeter-Derived Tides

The impact of applying corrections for the tide and/or surge, or tide–surge water-level variability on the quality of the estimated amplitudes and phases is assessed by comparing the VDs and their uncertainties of the corresponding scenarios to the 'No correction' scenario (see Table 3). The results are summarized in Tables 6 and 7 and Figures 4 and 5. From the results, we observe:

- Removing only the tidal signal has neither a positive effect on the estimated amplitudes and phases nor on their uncertainty (cf. 'No

Table 6. The VDs for the eight major tidal constituents, their RSS value, and the RSS17 or RSS93 value (depending on whether the EOT set or RWS set of constituents is used in the harmonic analyses, see Sect. 2.4) for all scenarios described in Table 3.

Scenario	Q1	O1	P1	K1	N2	M2	S2	K2	RSS8	RSS17	RSS93
Results for EOT constituent set											
No correction	1.22	1.29	0.94	1.41	0.87	1.21	1.25	1.25	3.70	5.57	
DAC	0.60	0.76	0.56	1.02	0.60	0.51	0.50	0.80	2.10	3.05	
FES tide	1.22	1.30	0.94	1.41	0.86	1.21	1.25	1.25	3.70	5.55	
DAC + FES tide	0.59	0.77	0.56	1.03	0.60	0.50	0.51	0.80	2.10	3.03	
DCSM surge	0.77	0.68	0.65	0.56	0.64	0.70	0.68	0.62	2.07	3.08	
DCSM tide	1.20	1.29	0.92	1.40	0.86	1.21	1.23	1.25	3.67	5.51	
DCSM surge + DCSM tide	0.76	0.68	0.62	0.56	0.64	0.69	0.65	0.63	2.03	2.99	
DCSM tide–surge	0.31	0.27	0.37	0.36	0.29	0.27	0.33	0.30	0.98	1.44	
Results for RWS constituent set											
No correction	1.23	1.33	1.05	1.41	1.00	1.19	1.29	1.24	3.80		13.81
DAC	0.73	0.87	0.54	1.03	0.63	0.49	0.50	0.82	2.19		7.65
FES tide	1.23	1.32	1.05	1.41	1.00	1.19	1.29	1.24	3.80		13.80
DAC + FES tide	0.73	0.87	0.54	1.00	0.63	0.49	0.50	0.82	2.18		7.64
DCSM surge	0.77	0.71	0.67	0.58	0.66	0.70	0.67	0.62	2.10		7.41
DCSM tide	1.23	1.32	1.04	1.40	0.99	1.18	1.28	1.25	3.79		13.74
DCSM surge + DCSM tide	0.75	0.71	0.65	0.57	0.67	0.68	0.67	0.62	2.07		7.30
DCSM tide–surge	0.32	0.28	0.36	0.41	0.31	0.27	0.34	0.30	1.01		3.86

All values are in centimeters and represent the mean over the N ensemble members.

Table 7. Standard deviations of the VDs for the eight major tidal constituents computed over the N ensemble members ($N = 100$), as well as the standard deviations over the RSS8 (SD_{RSS8}) and the RSS17 (SD_{RSS17}) or RSS93 (SD_{RSS93}) values (depending on whether the EOT set or RWS set of constituents is used in the harmonic analyses, see Sect. 2.4).

Scenario	Q1	O1	P1	K1	N2	M2	S2	K2	SD_{RSS8}	SD_{RSS17}	SD_{RSS93}
Results for EOT constituent set											
No correction	0.68	0.64	0.42	0.55	0.42	0.61	0.66	0.60	0.62	0.54	
DAC	0.32	0.35	0.30	0.34	0.26	0.24	0.26	0.34	0.36	0.41	
FES tide	0.68	0.65	0.42	0.55	0.42	0.60	0.67	0.60	0.62	0.54	
DAC + FES tide	0.31	0.35	0.31	0.34	0.26	0.24	0.26	0.34	0.37	0.42	
DCSM surge	0.39	0.29	0.33	0.30	0.27	0.39	0.34	0.30	0.36	0.38	
DCSM tide	0.68	0.64	0.40	0.55	0.43	0.59	0.67	0.60	0.63	0.54	
DCSM surge + DCSM tide	0.37	0.29	0.28	0.30	0.28	0.38	0.32	0.29	0.35	0.36	
DCSM tide–surge	0.15	0.12	0.20	0.17	0.16	0.14	0.14	0.15	0.16	0.19	
Results for RWS constituent set											
No correction	0.73	0.67	0.45	0.56	0.48	0.58	0.65	0.62	0.61		0.63
DAC	0.34	0.36	0.28	0.34	0.27	0.23	0.26	0.35	0.39		0.39
FES tide	0.73	0.67	0.45	0.55	0.48	0.58	0.65	0.62	0.60		0.63
DAC + FES tide	0.34	0.36	0.28	0.34	0.27	0.23	0.27	0.35	0.39		0.41
DCSM surge	0.40	0.34	0.31	0.31	0.32	0.37	0.34	0.30	0.37		0.44
DCSM tide	0.71	0.67	0.44	0.55	0.48	0.57	0.66	0.62	0.60		0.62
DCSM surge + DCSM tide	0.38	0.34	0.29	0.31	0.32	0.36	0.33	0.29	0.36		0.47
DCSM tide–surge	0.16	0.14	0.19	0.19	0.15	0.14	0.15	0.15	0.16		0.19

For the definition of the scenarios we refer to Table 3. All values are in centimeters.

correction' to 'FES tide' and 'DCSM tide'). This is regardless of whether the set of EOT or RWS is used in the tidal analysis.

- Removing only the surge signal has a positive impact. For the individual constituents, the reduction in VD is between 0.23 and 0.85 cm. Also, the uncertainties drop between 21% and 61%.

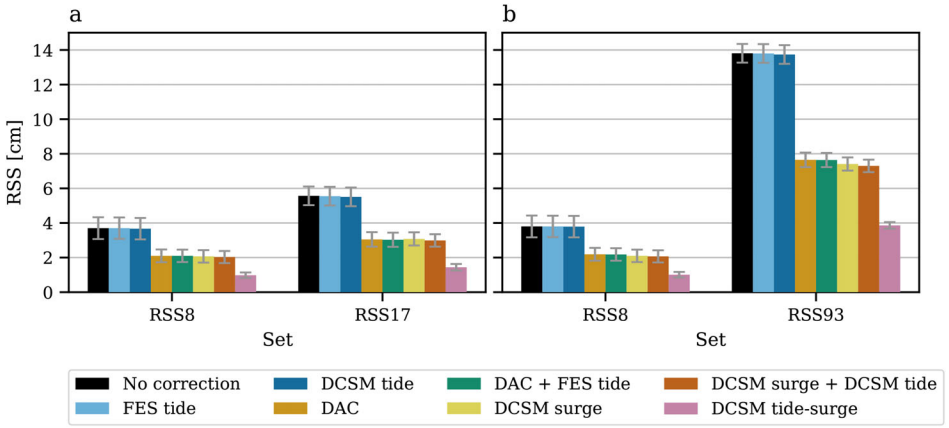

Figure 4. Summary of the results. RSS mean and 1-SD (error bar) computed over the *N* ensemble members ($N = 100$). (a) EOT set. (b) RWS set. For the definition of the scenarios, we refer to Table 3.

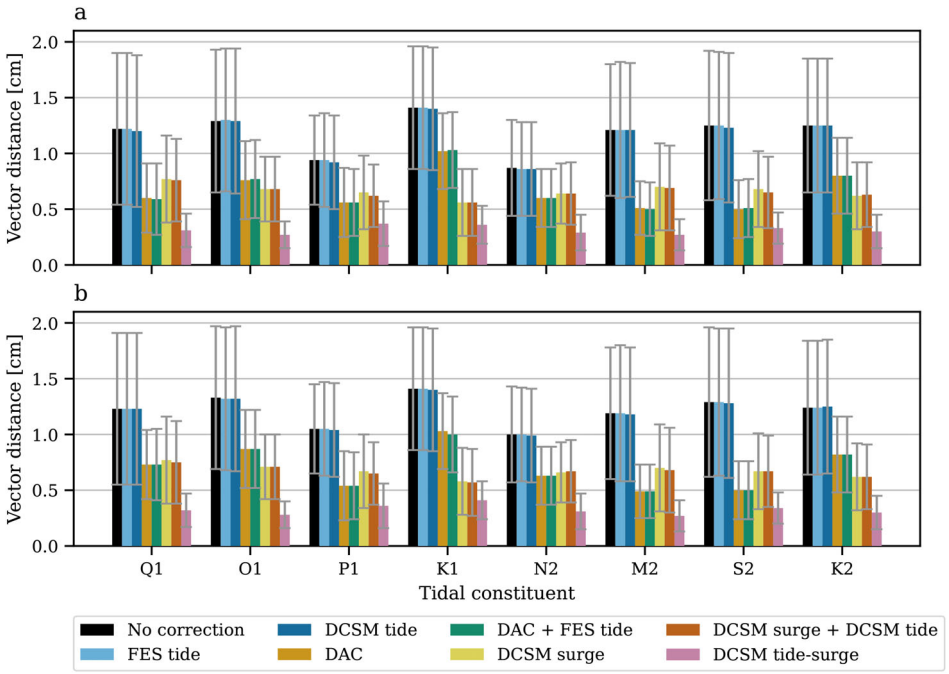

Figure 5. Summary of the results. VDs mean and 1-SD (error bar) for the eight major tidal constituents computed over the *N* ensemble members ($N = 100$). (a) EOT set. (b) RWS set. For the definition of the scenarios we refer to Table 3.

- The impact obtained when removing both tides and surge is comparable to the impact obtained when only the surge is removed if FES and DAC are used (cf. 'No correction' and 'DAC + FES tide' vs. 'No correction' and 'DAC') or the sum of DCSM-derived tides and DCSM-derived

surge (cf. 'No correction' and 'DCSM surge + DCSM tide' vs. 'No correction' and 'DCSM surge').
- A large improvement is observed in case the DCSM-derived tide–surge water levels are used, both in terms of VDs and RSS differences as well as in the uncertainties (cf. 'No correction' and 'DCSM tide–surge' vs. 'No correction' and 'DCSM surge + DCSM tide'). For the individual constituents, the reduction in VD is between 0.57 and 1.05 cm, while all uncertainties drop by more than 50%.
- For all scenarios, the uncertainties for the major eight constituents are between 33% and 60% of the VDs. This means that the timing of the altimeter observations has quite an impact on the estimated amplitudes and phases.

The removal of tide and surge water levels is a commonly applied pre-processing step. For instance, Hart-Davis et al. (2021) removes both the updated FES2014 and DAC to produce the EOT20 tide model. Our results confirm that removing the surge has a positive impact on the quality of altimeter-derived tides. This result is, indeed, well understood; removing the surge reduces the nontidal water-level variability and hence improves the signal-to-noise ratio. The removal of the tide does not seem to improve anything, no matter whether the EOT or RWS set of constituents is used in the analysis.

The Impact of Including the Non-linear Tide–Surge Interaction

To assess the impact of including the tide–surge interaction in removing the tide and surge water levels prior to the harmonic analysis, we compare scenario 'DCSM surge + DCSM tide' with 'DCSM tide–surge' (see Tables 6 and 7 and Figures 4 and 5). From the results, we observe:

- A reduction of the VDs for the 8 major constituents. The smallest reduction is observed for K1 (0.20 cm/0.16 cm for the EOT/RWS set). For the other constituents, the change is a least 0.25 cm, with the largest improvement for Q1 (0.45 cm, EOT set).
- The RSS8 drops with more than 50% from 2.03 to 0.98 cm (EOT set) and 2.07 cm to 1.01 cm (RWS set). The RSS17 and RSS93 dropped 51.8% and 47.1%, respectively.
- All uncertainties reduce between 28.6% (P1, EOT set) and 63.2% (M2, EOT set).

The obtained reductions are significant. Since we repeated the analysis both with the EOT and RWS sets of constituents, we can exclude the

possibility that the improvement is caused by the parametrization; for both sets, the results are quite similar. In fact, the controlled design of the experiment allows only one explanation; the improvement is due to the inclusion of the nonlinear tide–surge interaction. Because we saw earlier that this has a particularly large impact on the representation of M2 (see Sect. 3.1), we looked at whether it makes a difference when we replace the tidal component in the scenario 'DCSM surge + DCSM tide' with the tide obtained from a harmonic analysis of the tide–surge water levels. The short answer is no: the VDs and RSS values are similar to what we obtained in the case of the 'DCSM surge' scenario.

The RSS8 values obtained by Stammer et al. (2014) for FES2012 are 1.12 cm (deep ocean), 4.82 cm (European Shelf), and 7.50 cm (coastal waters). Of course, there is no point in comparing values at one tide gauge/location to values obtained over many tide gauges. Furthermore, we use FES2014. However, it is worth noting that only by taking tide–surge interaction into account the RSS8 at Europlatform reduces to the level (Stammer et al. 2014) obtained for the deep ocean.

Discussions and Conclusion

Satellite radar altimetry has made an enormous contribution to improving the quality of global ocean tide models, not only in the deep waters but also in the shelf and coastal waters. It is well understood and documented that the quality of the models in the latter waters generally lags behind the quality in deep waters; in shallow waters, the tide is more complex due to nonlinear dynamics. These nonlinear distortions cause the so-called shallow water tides of which most cannot be estimated from altimeter data although they need to be considered to get a proper representation of the tide. However, why the quality of the models for the eight major constituents is also significantly lower has, to our knowledge, never been explicitly investigated. In this study, we answered the question of whether this is due to the quality of the models used to remove tide and surge or the general approach to treat tide and surge as two separate components of the water level obtained from stand-alone models. Such an approach, indeed, ignores the nonlinear tide–surge interaction.

The results show that ignoring the nonlinear tide–surge interaction has a large impact on the quality of the altimeter-derived eight major tidal constituents. Expressed in the root-sum-square (RSS) of the eight vector differences (VDs), we obtained a reduction of more than 50% in the case we removed the DCSM tide–surge water levels compared to the case in which we removed the sum of the DCSM tide and DCSM surge water levels. The RSS obtained in the latter case was only 3.3% (EOT set) lower compared to

the case in which FES and DAC were used. This shows that (i) using a high-quality, high-resolution model is not necessarily beneficial, and (ii) the result cannot be explained by the fact that the Europlatform tide gauge has been used to calibrate the DCSM. We again would like to stress that none of the data used in this calibration has been used in our analyses. By repeating the analyses using a more complete set of tidal constituents than only the ones typically used in estimating altimeter tides, we showed that the impact is not caused by deficiencies in the parameterization. Apart from the improved fit to the control data, we observed a reduction of more than 60% for the M2 constituent.

Even though our analyses are limited to one location and based on 'partially synthetic' data, the results can be well understood. Indeed, including nonlinear interaction in applying corrections for tide and surge to the observed water levels prior to the harmonic analysis will significantly reduce the variance of the nonparameterized signal. This is known to have a strong impact on the estimated tides (Andersen 1999; Andersen et al. 2006). We, therefore, have no doubts that the main conclusion is indeed an important explanation for the lower quality of the major tidal constituents in shelf and coastal waters.

The main implication of our conclusion will be that instead of relying on separate corrections for tide and surge, combined tide–surge corrections are needed. These corrections can only be obtained using a time-stepping model and have to be provided with sufficient spatiotemporal resolution. This is manageable for regional studies, but to provide such corrections for the full record of altimeter data requires huge storage space. Apart from this, it seems unknown in which regions a combined tide–surge model exist (regional or global) that represents the combined signal with sufficient accuracy. A possible candidate model may be the Global Tide and Surge Model (Verlaan, Kleermaeker, and Buckman 2015; Muis et al. 2016; Wang et al. 2022).

Acknowledgement

This study was performed in the framework of the Versatile Hydrodynamics project, funded by the Netherlands Organization for Research (NWO). This support is gratefully acknowledged.

Disclosure statement

No potential conflict of interest was reported by the authors.

Data availability statement

The 2D DCSMv7 datasets related to this article can be found at https://doi.org/10.4121/21070933, an open-source online data repository hosted at 4TU.ResearchData (Guarneri et al. 2022). FES2014b and DAC datasets are available publicly through AVISO+ (https://www.aviso.altimetry.fr/).

References

Andersen, O. B. 1999. Shallow water tides in the northwest European shelf region from TOPEX/POSEIDON altimetry. *Journal of Geophysical Research: Oceans* 104 (C4):7729–7741.

Andersen, O. B., G. D. Egbert, S. Y. Erofeeva, and R. D. Ray. 2006. Mapping nonlinear shallow-water tides: A look at the past and future. *Ocean Dynamics* 56 (5–6):416–429.

Arns, A., T. Wahl, C. Wolff, A. T. Vafeidis, I. D. Haigh, P. Woodworth, S. Niehüser, and J. Jensen. 2020. Non-linear interaction modulates global extreme sea levels, coastal flood exposure, and impacts.*Nature Communications* 11 (1):1918–2041.

Carrère, L., Y. Faugère, and M. Ablain. 2016. Major improvement of altimetry sea level estimations using pressure-derived corrections based on ERA-Interim atmospheric reanalysis. *Ocean Science* 12 (3):825–842.

Carrère, L., Y. Faugère, E. Bronner, and J. Benveniste. 2011. Improving the dynamic atmospheric correction for mean sea level and operational applications of altimetry. In *Proceedings of the Ocean Surface Topography Science Team (OSTST) Meeting*, 2011, October 19–21. San Diego, CA, USA, 16–21.

Carrère, L, and F. Lyard. 2003. Modeling the barotropic response of the global ocean to atmospheric wind and pressure forcing – Comparisons with observations. *Geophysical Research Letters* 30 (6).

Carrère, L., F. Lyard, M. Cancet, A. Guillot, and L. Roblou. 2013. FES2012: A new global tidal model taking advantage of nearly 20 years of altimetry. In *Proceedings of the 20 Years of Progress in Radar Altimetry Symposium: 24 - 29 September 2012, Venice, Italy*, , ed. L. Ouwehand, vol. 710, 13. ESA Special Publication.

Cheng, Y, and O. B. Andersen. 2011. Multimission empirical ocean tide modeling for shallow waters and polar seas. *Journal of Geophysical Research: Oceans* 116 (C11).

Deltares. 2022. *D-flow flexible mesh – Computational cores and user interface – User manual (draft)*. Deltares, Delft, The Netherlands. Accessed June, 2013. https://content.oss.deltares.nl/delft3d/manuals/D-Flow_FM_User_Manual.pdf.

Egbert, G. D, and S. Y. Erofeeva. 2002. Efficient inverse modeling of Barotropic Ocean tides. *Journal of Atmospheric and Oceanic Technology* 19 (2):183–204.

Guarneri, H., M. Verlaan, D. C. Slobbe, J. Veenstra, F. Zijl, J. Pietrzak, S. M. L. Keyzer, Y. Afrasteh, and R. Klees. 2022. Tide-surge, tide and surge simulations output of 2D DCSM-FM V7 from 1980 to 2020 at euro platform.

Hart-Davis, M. G., G. Piccioni, D. Dettmering, C. Schwatke, M. Passaro, and F. Seitz. 2021. EOT20: A global ocean tide model from multi-mission satellite altimetry. *Earth System Science Data* 13 (8):3869–3884.

Hersbach, H., B. Bell, P. Berrisford, S. Hirahara, A. Horányi, J. Muñoz-Sabater, J. Nicolas, C. Peubey, R. Radu, D. Schepers, et al. 2020. The ERA5 global reanalysis. *Quarterly Journal of the Royal Meteorological Society* 146 (730):1999–2049.

Horsburgh, K. J, and C. Wilson. 2007. Tide-surge interaction and its role in the distribution of surge residuals in the North Sea. *Journal of Geophysical Research* 112 (C8):C08003.

Idier, D., X. Bertin, P. Thompson, and M. D. Pickering. 2019. Interactions between mean sea level, tide, surge, waves and flooding: Mechanisms and contributions to sea level variations at the coast. *Surveys in Geophysics* 40 (6):1603–1630.

Idier, D., F. Dumas, and H. Muller. 2012. Tide-surge interaction in the English Channel. *Natural Hazards and Earth System Sciences* 12 (12):3709–3718.

Johns, B., A. D. Rao, S. K. Dube, and P. C. Sinha. 1985. Numerical modelling of tide-surge interaction in the Bay of Bengal. *Philosophical Transactions of the Royal Society of London Series A* 313 (1526):507–535.

Le Provost, C., M.-L. Genco, and F. Lyard. 1995. *Modeling and predicting tides over the world ocean*, In *Quantitative Skill Assessment for Coastal Ocean Models*, ed. D. R. Lynch, A. M. Davies, 175–201. Washington, D. C.: American Geophysical Union (AGU).

Leendertse, J. J. 1967. *Aspects of a computational model for long-period water-wave propagation*. Santa Monica, California: The Rand Corporation for the United States Air Force Project Rand.

LEGOS/CNRS/CLS. 1992. URL. Dynamic atmospheric correction. https://www.aviso.altimetry.fr/en/data/products/auxiliaryproducts/dynamicatmospheric-correction.html. Accessed March 10, 2022.

Lyard, F., F. Lefevre, T. Letellier, and O. Francis. 2006. Modelling the global ocean tides: Modern insights from FES2004. *Ocean Dynamics* 56 (5–6):394–415.

Lyard, F. H., D. J. Allain, M. Cancet, L. Carrère, and N. Picot. 2021. FES2014 global ocean tide atlas: Design and performance. *Ocean Science* 17 (3):615–649.

Muis, S., M. Verlaan, H. C. Winsemius, J. C. J. H. Aerts, and P. J. Ward. 2016. A global reanalysis of storm surges and extreme sea levels.*Nature Communications* 7 (1):11969.

Ponte, R. M. 2006. Low-frequency sea level variability and the inverted barometer effect. *Journal of Atmospheric and Oceanic Technology* 23 (4):619–629.

Ponte, R. M., C. Wunsch, and D. Stammer. 2007. Spatial mapping of time-variable errors in Jason-1 and TOPEX/Poseidon sea surface height measurements. *Journal of Atmospheric and Oceanic Technology* 24 (6):1078–1085.

Prandle, D, and J. Wolf. 1978. The interaction of surge and tide in the North Sea and River Thames. *Geophysical Journal International* 55 (1):203–216.

Proudman, J. 1955a. The propagation of tide and surge in an Estuary. *Proceedings of the Royal Society of London Series A* 231(1184):8–24.

Proudman, J. 1955b. The effect of friction on a progressive wave of tide and surge in an estuary. *Proceedings of the Royal Society of London Series A* 233(1194):407–418.

Ralston, M. L, and R. I. Jennrich. 1978. Dud, a derivative-free algorithm for nonlinear least squares. *Technometrics* 20 (1):7–14. http://www.jstor.org/stable/1268154.

Ray, R. D. 1999. A global ocean tide model from TOPEX/POSEIDON altimetry: GOT99.2. Technical report, Goddard Space Flight Center, Greenbelt, NASA Tech. Memo 209478, 58.

Ray, R. D., G. D. Egbert, and S. Y. Erofeeva. 2011. Tide predictions in shelf and coastal waters: Status and prospects. In *Coastal altimetry*, ed. S. Vignudelli, A. Kostianoy, and J. Benveniste, 191–216. Berlin, Heidelberg: Springer Berlin Heidelberg.

Shum, C. K., P. L. Woodworth, O. B. Andersen, G. D. Egbert, O. Francis, C. King, S. M. Klosko, C. Le Provost, X. Li, J. Molines, et al. 1997. Accuracy assessment of recent ocean tide models. *Journal of Geophysical Research: Oceans* 102 (C11):25173–25194.

Stammer, D., R. D. Ray, O. B. Andersen, B. K. Arbic, W. Bosch, L. Carrère, Y. Cheng, D. S. Chinn, B. D. Dushaw, G. D. Egbert, et al. 2014. Accuracy assessment of global barotropic ocean tide models. *Reviews of Geophysics* 52 (3):243–282.

Stelling, G. S. 1984. *On the construction of computational methods for shallow water flow problems*. PhD thesis, Delft University of Technology, Delft Rijkswaterstaat Communications 35.

Veenstra, J. 2022. hatyan: Tidal analysis and prediction. https://github.com/Deltares/hatyan, Version 2.5.62. Accessed July 18, 2022.

Verlaan, M., S. De Kleermaeker, and L. Buckman. 2015. *GLOSSIS: Global storm surge forecasting and information system*. https://doi.org/10.3316/informit.703696922952912.

Vignudelli, S., F. Birol, J. Benveniste, L.-L. Fu, N. Picot, M. Raynal, and H. Roinard. 2019. Satellite altimetry measurements of sea level in the coastal zone. *Surveys in Geophysics* 40 (6):1319–1349.

Vignudelli, S., A. G. Kostianoy, P. Cipollini, and J. Benveniste. 2011. *Coastal altimetry*, 1st ed. Springer-Verlag, Berlin.

Wang, X., M. Verlaan, M. I. Apecechea, and H. X. Lin. 2022. Parameter estimation for a global tide and surge model with a memory-efficient order reduction approach. *Ocean Modelling* 173:102011.

Zaron, E. D, and S. Elipot. 2021. An assessment of global ocean barotropic tide models using geodetic mission altimetry and surface drifters. *Journal of Physical Oceanography* 51 (1):63–82.

Zhang, W.-Z., F. Shi, H.-S. Hong, S.-P. Shang, and J. T. Kirby. Jun 2010. Tide-surge interaction intensified by the Taiwan Strait. *Journal of Geophysical Research: Oceans* 115 (C6): C06012.

Zijl, F, and J. Groenenboom. 2019. Development of a sixth-generation model for the NW European Shelf (DCSM-FM 0.5nm). Technical report, Deltares. Available online at: https://publications.deltares.nl/11203715_004.pdf. Accessed July 18, 2022.

Zijl, F., J. Sumihar, and M. Verlaan. 2015. Application of data assimilation for improved operational water level forecasting on the northwest European shelf and north sea. *Ocean Dynamics* 65 (12):1699–1716.

Zijl, F., M. Verlaan, and H. Gerritsen. 2013. Improved water-level forecasting for the northwest European shelf and north sea through direct modelling of tide, surge and non-linear interaction. *Ocean Dynamics* 63 (7):823–847.